ECMWF COPERNICUS REPORT

Copernicus Climate Change Service

Product User Guide and Specification

Sea Ice Thickness Version 3.0

Issued by: Alfred Wegener Institute / Stefan Hendricks

Date: 17/04/2023

Ref: WP2-FDDP-2022-09_C3S2-Lot3_PUGS-of-v3.0-SeaIceThickness-products_v3.1

Official reference number service contract:

2021/C3S2_312a_Lot3_METNorway/SC1

Please cite as: Hendricks, S., Paul S. (2023) Sea Ice Thickness Version 3.0: Product User Guide and Specification. Copernicus Climate Change Service, Document reference: WP2-FDDP-2022-09_C3S2-Lot3_PUGS-of-v3.0-SeaIceThickness-products_v3.1.

Contributors

ALFRED WEGENER INSTITUTE
Stefan Hendricks
Stephan Paul

History of modifications

Version	Date	Description of modification	Chapters / Sections
1.0	30/04/2018	Initial Version	
1.1	30/05/2018	Modifications after technical comments by ECMWF	Corrections throughout the document
1.2	30/06/2019	Annual update	1.1.1: Corrected NRT timeliness to that of sea ice type ICDR 2.1: Added CDS as primary data download option Correction of document typos
1.3	11/09/2019	Modifications after technical comments by ECMWF and update of input data version.	1.1.1: ICDR timeliness is 33 days from 10/2019 on 1.1.1: Update of new CryoSat-2 input data version from 10/2019 on Minor corrections throughout the document 2.2: Removed description of Godiva visualization service (non C3S service)
1.4	25/06/2020	Annual update. Minor editorial corrections.	
2.0	02/07/2021	Major update for release of CDR version 2.0	All sections: General improvements of text and figures 1.1 Updates for CDR v2.0 1.2 Updates from CDR v2.0, reorganization of the subsections and updates from PQAD v2.0 1.3.1 Updates for CDR v2.0 1.3.2 Added description of CDR v2.0 anomaly in Envisat stream. 1.3.3 Added advisory for the computation of SIT trends. 2.0 Updated for CDR v2.0
2.1	23/07/2021	Update of validation results after reprocessing of Envisat part of CDR.	1.2: Updated figures and validation as well as stability results
2.2	30/09/2021	Feedback from ECMWF	Editorial changes in all sections Expanded Executive Summary 1.1 Added algorithm upgrade details
3.0	28/02/2023	Update for SIT-v3.0	All sections

Version	Date	Description of modification	Chapters / Sections
3.1	17/04/2023	Document amended in response to feedback from independent review, and finalised for publication	All sections

List of datasets covered by this document

Deliverable ID	Product title	Product type (CDR, ICDR)	Version number	Delivery date
WP2-FDDP-2022-09	Gridded Northern hemisphere Sea Ice Thickness Climate Data Record	CDR	v3.0	15/05/2021
WP2-ICDR-SIT-v1.0	Gridded Northern hemisphere Sea Ice Thickness Interim Climate Data Record	ICDR	v3.0	30/06/2021 - present time

Related documents

Reference ID	Document
D1	Hendricks, S., Paul, S. (2023) Sea Ice Thickness, Version 3.0: Algorithm Theoretical Basis Document. Copernicus Climate Change Service. Document reference WP2-FDDP-2022-09_C3S2-Lot3_ATBD-of-v3.0-SeaIceThickness-products_v4.1.
D2	Hendricks, S. (2023) Sea Ice Thickness Version 3.0: Product Quality Assessment Report. Copernicus Climate Change Service, Document reference: WP2-FDDP-2022-09_C3S2-Lot3_PQAR-of-v3.0-SeaIceThickness-products_v3.1.
D3	Kreiner, M-B., Dybkjær, G., Howe, E., Hendricks, S., Aaboe, S. (2023) Sea Ice: Target Requirements and Gap Analysis Document. Copernicus Climate Change Service, Document ref. WP3-TR-GAP-2022_C3S2-Lot3-TR-GAP-SeaIce-products_v2.1.

Acronyms

Acronym	Definition
AEM	Airborne Electromagnetic Induction Sounding
ATBD	Algorithm Theoretical Basis Document
C3S	Copernicus Climate Change Services
CDR	Climate Data Record
CDS	(Copernicus) Climate Data Store
CF	Climate & Forecast file format conventions
CryoSat-2	CryoSat-2 – ESA Earth Explorer Mission
EASE2	Equal-Area Scalable Earth Grid in version 2
ECMWF	European Centre for Medium-Range Weather Forecasts
ECV	Essential Climate Variable
Envisat	Environmental Satellite
ERS	European Remote Sensing Satellite (ERS-1, ERS-2)
ESA	European Space Agency
FRB	Freeboard
GCOS	Global Climate Observing System
ICDR	Interim Climate Data Record
ML	Machine-Learning (Method)
netCDF	Network Common Data Form (File Format)
NRT	Near real time
OSI-SAF	Ocean and Sea Ice Satellite Application Facility
RA-2	Radar Altimeter 2 (Envisat radar altimeter sensor)
RFRB	Radar Freeboard
RMSE	Root Mean Square Error
SAR	Synthetic Aperture Radar
SARin/SIN	Synthetic Aperture Radar Interferometric Mode
SGDR	Sensor Geophysical Data Record
SIC	Sea Ice Concentration
SIRAL	SAR Interferometric Radar Altimeter (CryoSat-2 main sensor)
SIT	Sea Ice Thickness
SIType	Sea Ice Type (first-year / multi-year sea ice)
SLA	Sea level anomaly
SSH	Sea surface height
TFMRA	Threshold first maximum retracker algorithm
ULS	Upward Looking Sonar
WGS84	World Geodetic System 1984
WMO	World Meteorological Organization

General definitions

The sea ice thickness CDR/ICDR is based on the evaluation of radar altimeter data. The thickness retrieval is an indirect process with several intermediary geophysical variables involved. The variables that are referred to throughout the document are defined in the following table.

Radar Range	The distance in meters between spacecraft and the dominant radar reflecting interface on the surface. This value is computed from the two-way delay time with the speed of light in a vacuum.
Surface Elevation	The elevation of the surface with respect to the WGS84 ellipsoid. Calculated as the ellipsoidal altitude of the spacecraft minus the radar range over different surface types.
Sea Surface Height/Elevation	The surface elevation of the sea level along the satellite ground track. Over sea ice, this value is based on spatial interpolation between direct observations at fracture or leads between ice floes.
Ice Surface Elevation	The elevation of sea ice surfaces perceived by the radar altimeter. This value does not consider that the radar range needs to be corrected for a slower wave propagation speed in the snow layer on the ice surface. It is also based on the assumption that the snow/ice interface is the dominant reflector.
Radar Freeboard	The freeboard value sensed by the radar altimeter, e.g., the ice surface elevation minus sea surface elevation.
Sea Ice Freeboard	Sea ice freeboard is the mean height of the sea ice upper surface above the water surface in the horizontal domain. Sea ice means all ice floating in the sea which has formed from freezing sea water, rather than by other processes such as calving of land ice to form icebergs. This variable is based on radar freeboard with a range correction of the slower wave propagation speed in the snow layer.
Snow Depth on Sea Ice	Snow depth, or surface snow thickness, refers to the snow on the solid ground or on surface ice cover, but excludes, for example, falling snowflakes. "Thickness" means the vertical extent of a layer and is assumed to apply to the whole area of each horizontal domain.
Sea ice Thickness	Sea ice Thickness means the vertical extent of a layer. Sea ice means all ice floating in the sea which has formed from freezing sea water, rather than by other processes such as calving of land ice to form icebergs. The value refers to the mean thickness of the ice-covered part of the area or grid cell.

Data Processing Levels

The concept of data processing levels[1] is a common way in satellite remote sensing to designate different data products. Processing levels range from Level-0 (unprocessed sensor raw data) to Level-4 (analysed and potentially gap filled geophysical parameters).

L1B	(Level-1b) Calibrated sensor data at full resolution of the sensor with ancillary information.
L2P	(Level-2 pre-processed) L2P sea ice thickness data contains daily summaries along the ground tracks of the satellite at the resolution of the sensor.
L3C	(Level-3 collated) L3C product files contain sea ice thickness data on a spatio-temporal grid from a single satellite.
L4	(Level-4) Data sets created from the analysis of lower level data that result in gridded, gap-free products.

ECV requirements

An essential climate variable (ECV) is a variable, or group of variables that critically contributes to the characterization of the Earth Climate System (WMO, 2022). Requirements for an ECV product is expressed by 5 criteria:

Spatial Resolution	Horizontal and vertical (if needed).
Temporal resolution (or frequency)	The frequency of observations e.g. hourly, daily or annual.
Measurement Uncertainty	The parameter, associated with the result of a measurement, that characterizes the dispersion of the values that could reasonably be attributed to the measurand. It includes all contributions to the uncertainty, expressed in units of 2 standard deviations, unless stated otherwise.
Stability	The change in bias over time. Stability is quoted per decade.
Timeliness	The time expectation for accessibility and availability of data.

For each criterion, 3 values are defined that describe the maturity of an ECV product:

Goal	an ideal requirement above which further improvements are not necessary.
Breakthrough	an intermediate level between threshold and goal which, if achieved, would result in a significant improvement for the targeted application. The breakthrough value may also indicate the level at which specified uses within climate monitoring become possible. It may be appropriate to have different breakthrough values for different uses.
Threshold	the minimum requirement to be met to ensure that data are useful.

[1] https://www.earthdata.nasa.gov/engage/open-data-services-and-software/data-information-policy/data-levels [last accessed 5th December, 2022]

Table of Contents

Scope of the document

This document provides an overview of all aspects of the Copernicus Climate Change Service (C3S) sea ice thickness (SIT) Climate Data Record (CDR) and Interim Climate Data Record (ICDR) products produced using the version 3.0 algorithm. The first part summarizes key elements of the algorithm (see the Algorithm Theoretical Basis Document [D1] for more detail) and product quality assessment (see the Product Quality Assessment Report [D2] for more detail) with respect to the existing target requirements [D3] and states known limitations of the SIT data record.

The second part of the document contains the technical specifications of the products, with information on aspects such as file format and content, as well as how to access and visualize the product.

Executive summary

The sea ice thickness CDR/ICDR is based on radar altimeter data from the Envisat and CryoSat-2 missions. Version 3.0 of the CDR covers the period from October 2002 to October 2010 (Envisat) and November 2010 to April 2020 (CryoSat-2), while the ICDR is based on CryoSat-2 data and covers from October 2020 to the present date.

Key scientific facts: The CDR/ICDR consists of monthly gridded files for the northern hemisphere during winter time (October through April). Estimates of Sea ice thickness (SIT) are retrieved by measuring sea ice freeboard, the elevation of the sea ice surface above local sea level, along ground tracks of a satellite radar altimeter. Freeboard is then converted to SIT using auxiliary information on snow mass and sea ice density. The geographical coverage is limited to all latitudes <81.5N for the Envisat and <88N for the CryoSat-2 mission timeframes. Data from all orbits within a month is gridded without gap filling or interpolation. SIT uncertainty and precision derived from CryoSat-2 data are considerably better than results derived from Envisat, despite a fairly low intermission bias (3 cm).

Important note for the computation of Arctic sea ice thickness trends
SIT is underestimated considerably (0.5 m) with respect to validation data before 2008. The full spatial extent of this underestimation is unknown as validation data is geographically limited. However, sea ice thickness trends computed from the C3S sea ice thickness CDR/ICDR version 3.0 must be considered as too small.

Algorithm Update: Version 3.0 improves spatial coverage due to improved handling of radar altimeter data of thin sea ice and in the marginal ice zone. The Envisat/CryoSat-2 intermission bias is notably reduced with respect to version 2.0 of the CDR by a new neural-network based waveform retracking approach.

Key technical facts: The monthly gridded Level-3 product is available as netCDF-4 files compliant with Climate & Forecast (CF) conventions and contains SIT, uncertainty and a status and quality flag of the SIT retrieval. The data is hosted on the C3S Climate Data Store[2].

[2] https://cds.climate.copernicus.eu/cdsapp#!/dataset/satellite-sea-ice-thickness (last accessed March 2023)

1. Sea Ice Thickness (SIT)

1.1 Product description

1.1.1 Primary Data

The primary observational data set for the Copernicus Climate Change Service (C3S) sea ice thickness (SIT) product is radar altimeter data from the Envisat and CryoSat-2. The CDR/ICDR is based on data from Envisat between October 2002 and October 2010 and CryoSat-2 since November 2011. Envisat data from the Envisat/CryoSat-2 overlap period between November 2010 and March 2012 is not included in the CDR. However, it is internally available for product quality control (See the Product Quality Assessment Report, PQAR [D2]).

Both sensors allow the determination of sea-ice freeboard along the nadir locations of the satellite's trajectory (see Figure 1). The retrieval is based on range measurements over both sea-ice surfaces and open water in leads between ice floes, that are converted to surface elevation using the known altitude of the satellite. First, the elevation measurements over open water are used to create an instantaneous sea surface elevation along the satellite's ground track. Then, sea-ice freeboard is derived by taking the difference between the sea-ice surface elevations and the interpolated sea surface from the previous step. Additional corrections are necessary to account for small scale sea surface variations and the role of snow on sea ice surface elevations. While this capability was demonstrated with radar data from pulse-limited radar altimeters such as those onboard the Envisat platform for sea ice in the Arctic (Laxon et al. 2004), only the CryoSat-2 mission had the retrieval of sea ice freeboard, and subsequently SIT, as a primary mission objective. Therefore, CryoSat-2 had been inserted into an orbit that allows sea ice observations at higher latitudes than Envisat, and it was equipped with an advanced radar altimeter system that enables the sea-ice freeboard to be determined at a higher spatial resolution and improved accuracy.

Input parameters required for the SIT retrieval consist of calibrated sensor data at full sensor resolution (Level-1b information), as well as the following data flags and fields required to correct for wave propagation delays in the atmosphere and tidal affects:

1. Geolocated radar echo return power (radar waveform)
2. Sensor altitude and orientation
3. Geophysical atmospheric range corrections
4. Tide corrections
5. Surface type flag (land, marine, land ice)
6. Data quality flags.

The input data products for both platforms are provided by the European Space Agency (Table 1).

Table 1: Primary observational data products for the sea ice thickness CDR/ICDR.

Platform	Sensor	Source	Processing Level	Timeliness	Target	Coverage
Envisat	RA-2	ESA	Sensor Geophysical Data Record (SGDR) (v3.0)	reprocessed (final)	CDR	Northern hemisphere (50N < lat < 81.45N) 2002/10 – 2012/03
CryoSat-2	SIRAL	ESA	Level-1B (SAR/SARin) Baseline-D	reprocessed (1 month)	CDR	Northern hemisphere (50N < lat < 88N) 2010/11 – on-going
				REP (33 days)	ICDR	

The RA-2 and SIRAL sensors, for Envisat and CryoSat-2 respectively, are both radar altimeters operating at Ku-Band (approx. 13.5 GHz). However, they operate in different modes. Envisat's RA-2 is a pulse limited radar altimeter, while CryoSat's SIRAL uses a Synthetic Aperture Radar (SAR) system to improve the spatial resolution of the radar pulse.

1.1.1.1 Envisat

The Environmental Satellite (Envisat) mission was launched on board an Ariane-5 launch system on 28 February 2002 and failed on 08 April 2012, after 10 years of activity. One of the nine sensors onboard Envisat was the pulsed radar RA-2, a successor of the ERS radar altimeters. The radar operated at two frequencies (Ku & S-Band), however only the Ku-Band data is used for the SIT retrieval.

Table 2: Envisat orbit specifications, and characteristics of the radar altimeter (RA) sensor.

Data Period	Northern winter month (full)	Oct 2002 – Mar 2012
Orbit	Repeat cycle	35-day 30-day (from 2010 onward)
	Altitude	800 km
	Inclination	98.55°
	Period	100.6 minutes
Radar Altimeter	Name	RA-2
	Wave band	13.575 GHz (Ku-Band) 3.2 GHz (S-Band) (failed in 2007)
	Type	Pulse-limited
	Footprint	2-10 km (depending on surface)

1.1.1.2 CryoSat-2

The CryoSat-2 satellite is a dedicated topography mission for cryosphere applications and the retrieval of SIT in the Arctic is one of the primary mission objectives. Thus, the orbit and radar altimeter are optimized for high-latitude observations at improved sensor resolution. The mission was launched in April 2010 and remains operational to this date.

Table 3: CryoSat-2 orbit specifications, and characteristics of the radar altimeter sensor.

Data Period	Northern winter month (full)	Nov 2010 – on-going
Orbit	Repeat cycle	369 days; 30-day sub-cycle
	Altitude	717 km
	Inclination	92.00°
	Period	100 minutes
Radar Altimeter	Name	SIRAL
	Wave band	13.575 GHz (Ku-Band)
	Type	Doppler-delay (SAR) Doppler-delay interferometric (SARin)
	Footprint	0.3 km x 1.6 km (along x across track)

1.1.2 Auxiliary Data

Auxiliary data sets are used to parametrize the SIT retrieval algorithm and to geographically mask parameters. The SIT product depends on a set of auxiliary parameters that consists of both static parameter fields and remote sensed geophysical parameters (shown in Table 4).

Table 4: Summary of auxiliary data sources, and key characteristics, used for the SIT retrieval.

Auxiliary Type	Description	Target	Temporal Resolution	Coverage	Used for
Mean Sea Surface Height (MSS)	DTU21: Gridded mean sea surface height from multi-sensor altimetry data	CDR, ICDR	Static	Global Oceans	Sea surface height interpolation
Sea Ice Concentration (SIC)	EUMETSAT OSI-SAF SIC CDR v3.0 (OSI-450)	CDR	daily	Northern hemisphere	Surface type classification Data masking
	EUMETSAT OSI-SAF SIC ICDR v3.0 (OSI-430-b)	ICDR			
Sea Ice Type (SIType)	C3S SIType CDR v3.0	CDR	daily	Northern hemisphere	Sea ice density parametrization Snow climatology modification
	C3S SIType ICDR v3.0	ICDR			

Table 4 (continued): Summary of auxiliary data sources, and key characteristics, used for the SIT retrieval.

Auxiliary Type	Description	Target	Temporal Resolution	Coverage	Used for
Snow on Sea Ice (SNOW)	Climatology of snow depth and snow density from merged Warren climatology and AMSR2 data	CDR, ICDR	Monthly (Static) with daily interpolation	Northern hemisphere	range corrections Archimedes principle

1.1.3 Algorithm

The retrieval of SIT from radar altimetry is based on the Archimedes Principle, as sea ice is in isostatic equilibrium except for an insignificant area of grounded sea ice in shallow regions. Thus, the thickness of the sea ice layer can be inferred from its height above sea level (known as the *sea ice freeboard*), together with snow depth and the densities of snow, sea ice and sea water.

The SIT algorithm is therefore separated in two essential parts:

1. Estimation of sea ice freeboard from radar range measurements along the ground track of the satellite, and
2. The conversion of the altimeter-derived sea ice freeboard to thickness using auxiliary information for snow mass as well as sea ice and sea water densities.

Satellite radar altimeters measure the echo power distribution, which is used to estimate the elevation of the main backscatter horizon in the nadir of the satellite position. The strategy to estimate sea ice freeboard consists of exploiting differential range measurements over sea ice and water in openings (leads) inside the ice cover. The lead elevation measurements are essential to estimate the instantaneous sea surface height at the time of the satellite overpass since the instantaneous sea surface height may deviate from mean sea level due to effect of tides or atmospheric pressure systems. The lead elevations then act as tie points for the interpolated along-track sea surface height, which is the reference surface for estimating freeboard from the sea ice elevations. This principle is illustrated in Figure 1 and the data processing scheme is shown in Figure 2. A sample waveform from the SIRAL instrument on board Cryosat-2 is shown in Figure 3.

The utility of this principle is limited to periods with cold conditions without snow melt processes or open melt ponds. Therefore, SIT retrieval from radar altimetry is limited to the period from October through to April for the Northern Hemisphere.

The following sections give a summary of the essential algorithm steps from the primary radar altimeter data to the gridded SIT fields and their uncertainty. For a full description of the algorithm, please refer to the Algorithm Theoretical Baseline Document [D1].

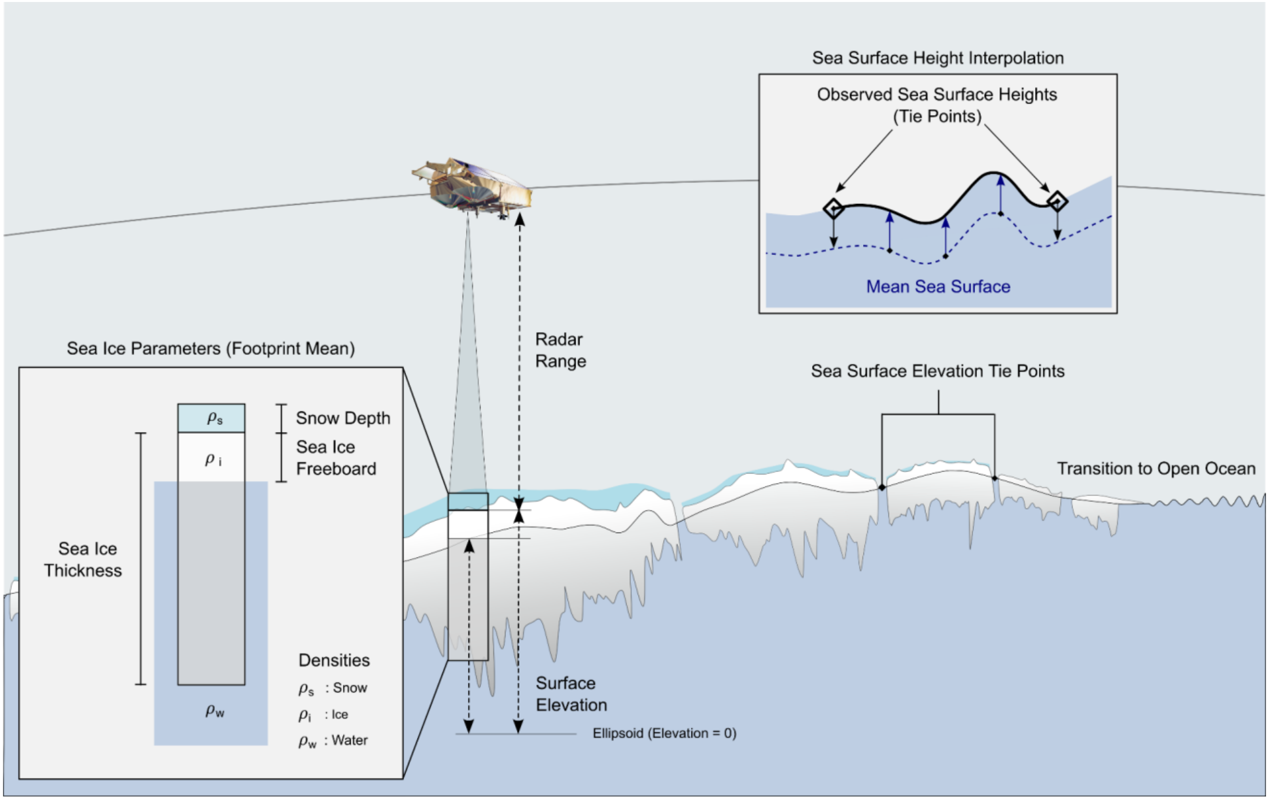

Figure 1: Principle of sea ice thickness retrieval using radar altimetry: Freeboard is derived as the difference between the surface elevations of sea ice and the sea surface, which are based on radar range measurements over both surface types. This step involves the interpolation of discrete sea surface elevation observations (tie points) in leads between ice floes. The interpolation is aided by a mean sea surface. Sea ice freeboard is then converted into sea ice thickness based on Archimedes Principle, considering snow depth and the densities of snow, sea ice and sea water.

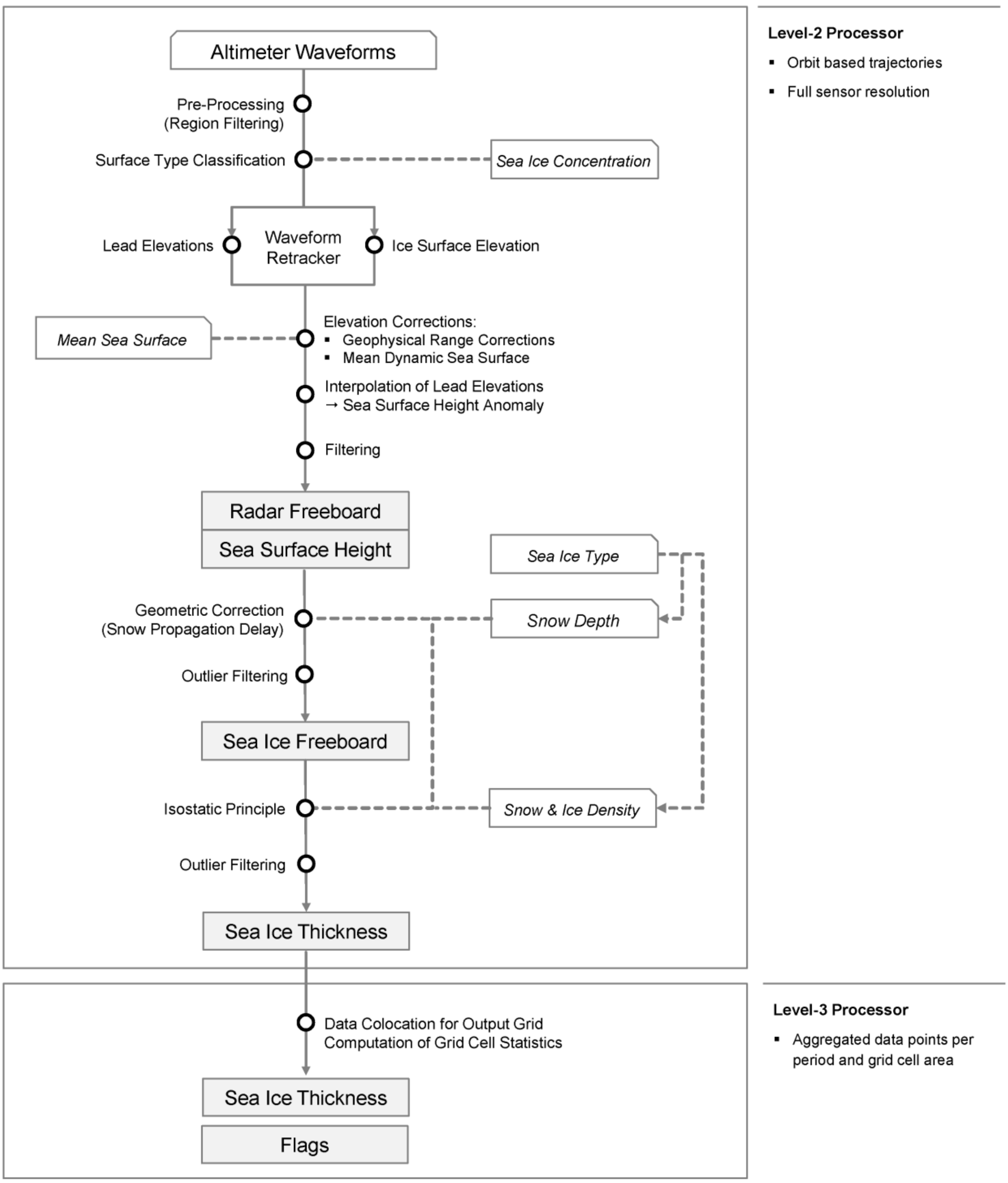

Figure 2: Processor workflow for SIT CDR v3.0. Sea ice thickness is estimated based on radar waveforms and auxiliary data for individual orbits in the Level-2 Processor. All Level-2 data sets for a given month is then aggregated and gridded in the Level-3 processor. For a comprehensive and detailed description of this workflow, see the Algorithm Theoretical Basis Document (ATBD, [D1]).

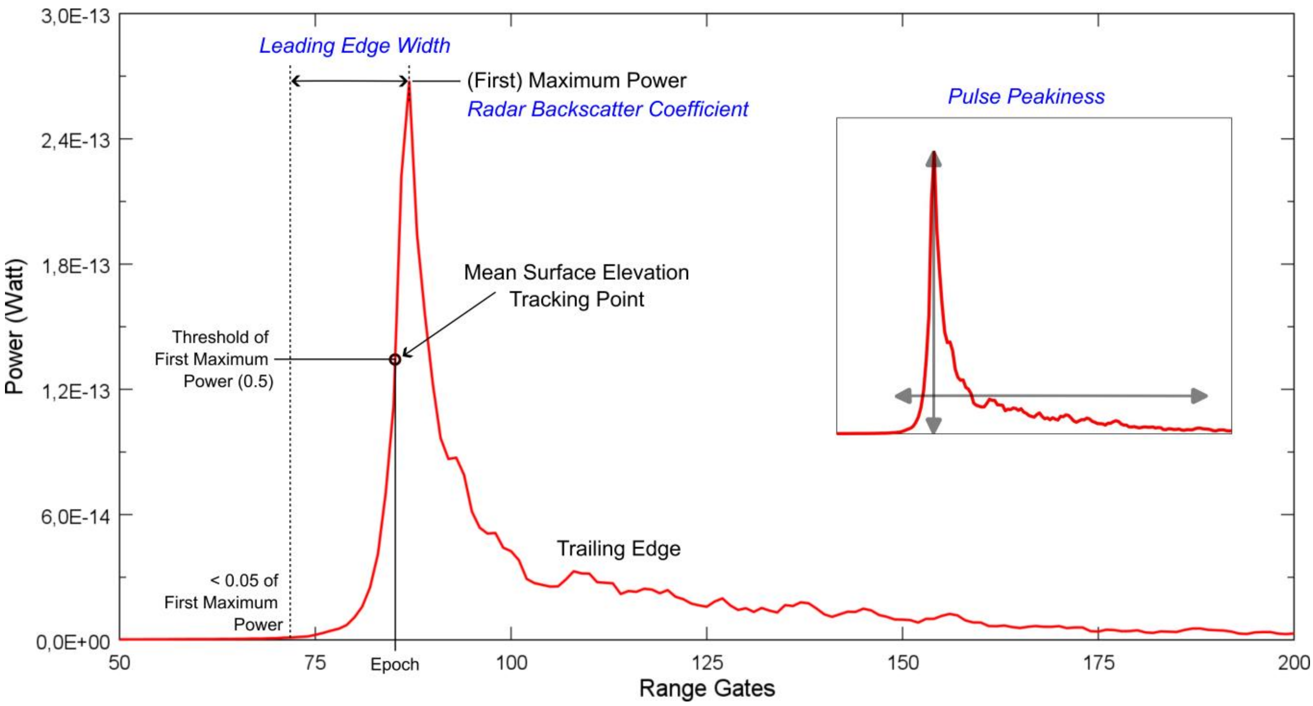

Figure 3: Radar waveform characterization for an example of a sea ice waveform from CryoSat-2 SIRAL data with 256 range gates in total. Each waveform is characterized by the leading-edge width, radar backscatter coefficient derived from the maximum power and pulse peakiness, which describes the ratio of peak to cumulative power. The mean surface elevation is estimated from the location where the leading edges exceeds a threshold, in this case 0.5 of the normalized (first) maximum power.

1.1.3.1 Surface Type Classification

The initial step for the estimation of sea surface height and freeboard is the surface type classification for individual radar echoes based on the echo (also known as the waveform) shape. The classification scheme recognizes four surface types:

1. Open ocean areas. Currently not used.
2. Lead/opening between ice floes used for sea surface height estimation.
3. Sea ice surface used for freeboard and thickness retrieval.
4. Mixed surface/unknown that are discarded from further processing.

The main factor for discrimination of especially lead and sea ice surface is the significant difference in backscatter properties that affect the shape of the radar waveform (Figure 3). While leads are specular targets with mainly reflection, the echo from sea ice surfaces is diffuse due to scattering because of the rougher surface. This affects the shape of return echo (waveform), and the classification is based on three parameters that describe the main shape of the waveform:

1. radar backscatter coefficient
2. pulse peakiness
3. leading edge width

The radar backscatter coefficient is an indicator of the strength of the backscattered signal, where specular reflections over leads are generally characterized with a larger backscatter coefficient value. The width of the leading edge is a proxy for the distribution of surface heights in the footprint. Meanwhile, the pulse peakiness is a parameter that combines the impact of backscatter coefficient and surface type variability in the footprint. The leading-edge quality is used to filter noisy waveforms.

In addition, a sea ice concentration mask (> 15%) is used to ensure the correct discrimination between sea ice and open ocean waveforms in cases of strong surface waves.

All three waveform shape parameters co-variate to a certain extent, but the combination was found most suitable to discriminate between specular (leads) and diffuse (ice surfaces) reflection targets (Paul et al., 2018).

Lead and open ocean waveforms are labeled in the beginning of the surface type classification scheme and the remaining waveforms in the sea ice mask are labeled as sea ice. An additional leading edge quality parameter is used as a filter. If the leading edge is too noisy, the surface type of the waveform is set to unknown and discarded from further processing.

1.1.3.2 Freeboard and Sea Level

The range from the satellite to the main backscatter horizon is determined for both open water and sea ice waveforms by an algorithm (TFMRA: Threshold first maximum retracker algorithm) that estimates the location (epoch) at the leading edge where the power has risen to a certain fraction (threshold) of the waveform´s peak power (Figure 3). Since the waveform shapes for Envisat and CryoSat-2 are inherently different, the threshold varies for surface type and platform as illustrated in Table 5.

Table 5: Retracker thresholds to estimate range for lead and sea ice surfaces.

Platform	Open Water Threshold	Sea Ice Threshold
Envisat	0.95 (static)	Neural network based, see below
CryoSat-2	0.5 (static)	0.5 (static)

The fixed thresholds are an empirical solution and only meant to be used in the combination of open water and sea ice retracker thresholds. They do not originate from a waveform forward model of different surface types.

In the case of Envisat pulse-limited waveforms, the larger impact of sea ice surface roughness on the leading edge does not allow a fixed retracker threshold to be defined. The retracker threshold is therefore determined from the waveform shape using a machine-learning (ML) approach. The model (Paul and Hendricks, 2022) has been trained to minimize the intermission bias between Envisat and CryoSat-2, using the overlap period of the two platforms between November 2010 and March 2012.

Freeboard is defined as the elevation of the sea ice surface above local sea level. Sea level, or sea surface height, cannot be determined continuously due to the presence of sea ice and needs to be interpolated between individual lead tie point elevations.

To minimize sea surface height (ssh) interpolation errors in areas with sparse tie point coverage, the lead elevation is referenced to the mean sea surface height which eliminates the main sea level variations. The interpolation of the residual elevations then yields the sea surface height for the full orbit segment, as an anomaly with respect to the mean sea surface height:

$$ssh = mss + sla \qquad \text{Eq 1}$$

Where:

mss = the Mean Sea Surface, and
sla = the Sea Level Anomaly.

The initial radar-derived freeboard is then obtained by subtracting the sea surface height from the sea ice elevation.

$$rfrb = elev_{sea\ ice} - ssh \qquad \text{Eq 2}$$

Where:

$rfrb$ = the Radar Freeboard e.g., the freeboard sensed by a radar altimeter,
$elev_{sea\ ice}$= the elevation of sea ice surfaces.

To avoid interpolation errors, any radar-derived freeboards further than 200km from the next sea surface height tie point are discarded.

The final step for the freeboard retrieval is a geometric correction that accounts for the slower wave propagation speed of the radar signal in the snow layer. It is assumed that the main scattering horizon for Ku-Band radar under dry and cold conditions is the snow/sea ice interface (see section 1.3.2.1).

$$frb = rfrb + \Delta r_{WP} \qquad \text{Eq 3}$$

Where:

frb = sea ice freeboard,
Δr_{WP}= range correction based on snow depth and snow density (Mallett et al, 2020)

Freeboard retrieval is therefore only valid in the northern winter months from October through April, as the effect of melting or partially melting snow on the radar range retrieval is still poorly understood. In addition, the presence of open melt ponds is a severe complication for unambiguous surface type classification.

1.1.3.3 Freeboard to Thickness Conversion

The freeboard to thickness conversion requires snow mass (depth and density) as well as sea ice density and sea water density as auxiliary information. Since snow on sea ice is not a routinely observed parameter, monthly climatological parameters for both depth and density are used as input. The snow depth climatology is based on field observations (Warren et al. 1999) and data from passive microwave remote sensing, and takes the lower snow depth over first year sea ice into account [D1]. The snow density climatology is based on a uniform increase of density over the winter season.

The knowledge of sea ice density also only extends to mean values for first year (FYI) and multi-year sea ice (MYI) from a limited number of observations (Alexandrov et al., 2010). Sea ice density is therefore a parameterization based on the C3S sea ice type CDR/ICDR[3], while a fixed value is used for the sea water density:

Table 6: Densities for the sea ice freeboard to thickness conversion

	Density (kg/m^3)
Sea Water	1024.0
First-year sea ice	916.7
Multi-year sea ice	882.0
Snow	Climatological values

The estimation of SIT from freeboard is then obtained from the assumption of hydrostatic equilibrium:

$$SIT = \frac{sd \times \rho_S - frb \times \rho_W}{\rho_W - \rho_I} \qquad \text{Eq 4}$$

Where:

SIT = sea ice thickness,
sd = snow depth,
ρ_S = snow density,
frb = sea ice freeboard,
ρ_W = sea water density,
ρ_I = sea ice density

The thickness algorithm is applied to each waveform, yielding a SIT profile (Level-2) along the satellite ground track. To exclude outliers, a threshold filter is applied with different parametrizations for Envisat and CryoSat-2 (Table 7).

[3] https://cds.climate.copernicus.eu/cdsapp#!/dataset/satellite-sea-ice-edge-type [Last accessed April 2023]

Table 7: Sea ice thickness along-track outlier filter settings

Platform	Valid along-track thickness (Level-2)
Envisat	-1 to 11 m
CryoSat-2	-0.5 to 10.5 m

1.1.3.4 Uncertainties

The uncertainties are computed for each data record via error propagation and the assumption that the error of sea water density is negligible:

$$\sigma_{sit} = \sqrt{\left(\frac{\rho_w}{\rho_w - \rho_i}\sigma_{frb}\right)^2 + \left(\frac{frb \cdot \rho_w + sd \cdot \rho_i}{\rho_w - \rho_i}\sigma_\rho^i\right)^2 + \left(\frac{\rho_s}{\rho_w - \rho_i}\sigma_{sd}\right)^2 + \left(\frac{sd}{\rho_w - \rho_i}\sigma_\rho^s\right)^2} \quad \text{Eq 5}$$

A full description of the error contributions of the individual parameter is given in [D1].

1.1.3.5 Grid Colocation

For the data collocation to the spatial grid, all Level-2 sea ice thickness values for a corresponding grid cell in the timeframe of one calendar month are averaged. This is done if a minimum number of 2 Level-2 data points are present.

Because the averaging impacts the uncertainty, the error propagation (Eq 5) is evaluated on grid-level to separate the effect of gridding on random and systematic error contributions. Random errors, such as the range noise for individual waveforms, will be reduced by averaging over all waveforms in a grid cell. Meanwhile, other error contributions such as snow load error or ice density error have correlation lengths larger than the 25km grid cell size. Thus, the uncertainty of gridded (Level-3) data is computed as:

$$\sigma_{l3,sit} = \sqrt{\left(\frac{\bar{\rho}_w}{\bar{\rho}_w - \bar{\rho}_i}\sigma_{l3,frb}\right)^2 + \left(\frac{\overline{frb} \cdot \bar{\rho}_w + \overline{sd} \cdot \bar{\rho}_i}{\bar{\rho}_w - \bar{\rho}_i}\bar{\sigma}_\rho^i\right)^2 + \left(\frac{\bar{\rho}_s}{\bar{\rho}_W - \bar{\rho}_i}\bar{\sigma}_{sd}\right)^2 + \left(\frac{\overline{sd}}{\bar{\rho}_W - \bar{\rho}_i}\bar{\sigma}_\rho^s\right)^2} \quad \text{Eq 6}$$

Where:

$\overline{var}$ = mean variable (e.g. $\overline{sd}$ is the mean of all Level-2 snow depth points in one grid cell)

with the freeboard uncertainty computed as:

$$\sigma_{l3,frb} = \sqrt{\left(\Delta r_{WP} \cdot \bar{\sigma}_{sd}\right)^2 + \left(\hat{\sigma}_{rfrb}\right)^2} \quad \text{Eq 7}$$

Random error components ($\hat{\sigma}$) are computed from the weighted mean error of the individual uncertainties of all data points in a grid cell:

$$\hat{\sigma} = \sqrt{\sum_{n_{L2}} \frac{1}{(\sigma_{L2})^2}}^{-1} \qquad \text{Eq 8}$$

while the uncertainty of systematic error contributions ($\bar{\sigma}$) are based on the average of the individual uncertainties of all data points in a grid cell.

The grid used for Level-3 data is an Equal-Area Scalable Earth Grid in version 2 (EASE2), which is based on a polar aspect spherical Lambert azimuthal equal-area projection (Brodzik et al., 2012) and the WGS84 ellipsoid. The grid dimension is 5400 km x 5400 km with a spatial resolution of 25 km, resulting in a 432 x 432 grid. The grid is centered on the geographic Pole, meaning that the Pole is located at the intersection of center cells (Figure 4)

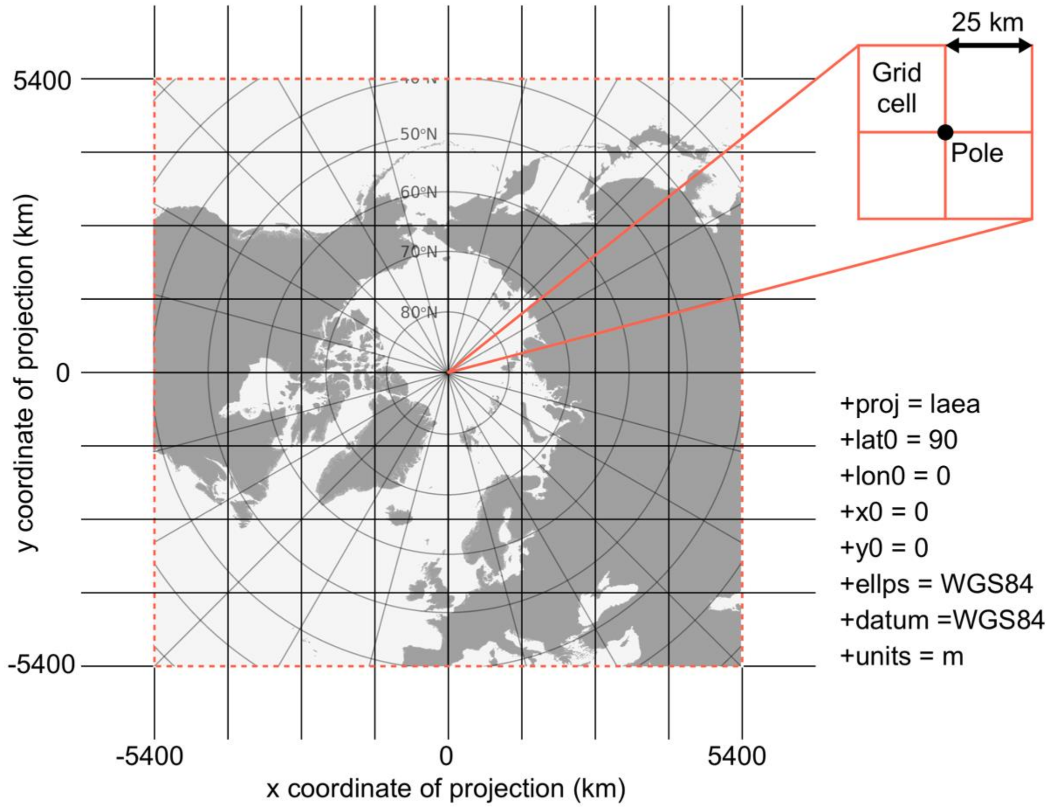

Figure 4: Specifications of the EASE2 25 km grid used for the C3S sea ice thickness ICDR/CDR.

1.1.4 Algorithm Heritage and Development

Version 3.0 of the C3S SIT CDR/ICDR replaces the previous version 2.0 and includes updates to the input data, the sea ice thickness retrieval algorithm, and the file format.

1. New surface type classification scheme for Envisat and CryoSat-2 improving the number of usable waveforms, especially in regions with the presence of thin sheet ice.
2. New neural-network based estimation of the sea ice retracker threshold, significantly reducing the Envisat/CryoSat-2 intermission bias found in version 2.0 of this dataset.
3. Update of sea ice concentration and type auxiliary data to Version 3.0 of the respective CDR/ICDR's.
4. Improved sea level anomaly estimation in areas with high-frequency fluctuations of the sea level, by replacing inverse barometric range correction with dynamic atmosphere range correction.
5. Minor changes to variable attributes and flag values.

These changes have the following impact on SIT with respect to version 2.0 of the CDR:

1. Improved geographical coverage of SIT, especially in the marginal ice zone. Better characterization of thin sea ice.
2. Minimal improvement in CryoSat-2 validation metrics (Section 1.1.1).
3. Degradation in Envisat validation metrics prior to 2008 (Section 1.1.1).
4. Improved precision of Envisat data (Section 1.2.2).
5. Improved consistency between CryoSat-2 and Envisat (Section 1.2.3.1).

1.1.5 Processing Level

The radar altimeter processing chain generates Level-2 (trajectories) and Level-3 (gridded) SIT information. The SIT CDR/ICDR made available to users is comprised of monthly Level-3 data only (Figure 4) and the Level-2 data is used internally for quality control. Possible distribution of Level-2 sea ice thickness in a future service development depends on user feedback.

1.2 Target requirements

The target requirements for SIT have been defined in the 2022 GCOS ECVs Requirements (WMO, 2022). Also see the General definitions section of this document for the definition of the ECV criteria. A more detailed discussion on the target requirements can be found in [D3] and the scientific reference is given by Lavergne et al., 2022.

Table 8: Requirements for SIT climate data records (WMO, 2022) and estimate of achieved performance of this CDR.

	Horizontal Resolution	**Temporal Resolution**	**Timeliness**	**Uncertainty**
Goal	1 km	Daily Year-Around	1 days	0.05 m
Breakthrough	25 km Distribution, mean & median	Weekly – Monthly Year-Around	7 days	0.1 m
Threshold	50 km	Monthly Wintertime Only	30 days	0.25 m
SIT CDR v3.0	25 km mean	Monthly Wintertime Only	31 days (ICDR)	approx. 0.25 m - 0.5 m[4]

While the Version 3.0 SIT product meets the GCOS target requirements for horizontal and temporal resolution, it only provides a mean thickness and not a SIT distribution. The estimated product uncertainty is larger than the GCOS requirements for goal (ideal value), breakthrough (intermediate) and threshold (minimum) requirements specified in Table 8. No specification is given for the stability of the SIT time series.

Both stability and uncertainty have been evaluated by cross-comparison of satellite results during overlap periods and by validation with independent SIT observations. The following sections provide a summary of the Product Quality Assurance Document [D2].

[4] Derived from validation exercise [D2]. Uncertainty estimates varies with validation data source.

1.2.1 Sea Ice Thickness Uncertainty & Bias

The uncertainty is estimated using independent SIT reference data sets. Three data sets are available that observe SIT nearly directly:

1. Airborne electromagnetic induction sounding (AEM) is a geophysical method that senses the sea ice plus snow thickness (total thickness) based on the contrast in electrical conductivity of sea ice and sea water. The AEM observations are converted into sea ice thickness by removing the snow depth used for the CDR.
2. AEM data in the combination with a snow radar provides true reference data for sea ice thickness. This data set has been collected during the IceBird aircraft campaigns by the Alfred Wegener Institute (Jutila et al, 2021a, Jutila et al, 2021b).
3. Upward looking sonar (ULS) sensors measure the draft of sea ice. This data set is converted into sea ice thickness by adding sea-ice freeboard used in the CDR.

Data from the reference sources is either temporally or spatially constrained and the conversion into SIT needs information on snow depth. In addition, the vast majority of airborne or moored SIT datasets originate from the western marginal seas of the Arctic Basin while the Eastern Arctic is under-represented.

For the SIT uncertainty assessment, AEM data from 12 airborne campaigns from 2007 to 2020, IceBird data from two airborne campaigns in 2017 and 2019, as well as ULS data from the Beaufort Gyre Exploration Project (BGEP) between 2003 and 2021 gridded to the product grid, are used. Snow depth and sea-ice freeboard from the satellite SIT product for the given month are used to convert the AEM & ULS observation to SIT for consistency reasons. The results in terms of Root Mean Standard Error (RMSE) and bias (satellite mean minus validation dataset) for all data points are summarized in Table 9. A detailed breakdown is given in [D2].

Table 9: Validation results for Envisat & CryoSat-2 SIT with AEM, IceBird and ULS reference observations. Bias is computed as satellite – reference. Values for all winter seasons are combined and presented.

Data Source	Metric	Envisat	CryoSat-2
AEM	RMSE (m)	0.88	0.74
	bias (m)	-0.71	-0.06
ULS	RMSE (m)	0.55	0.23
	bias (m)	-0.52	-0.10
IceBird	RMSE (m)	N/A	0.30
	bias (m)	N/A	-0.20
All	RMSE (m)	0.72	0.58
	bias (m)	-0.62	-0.11

The evaluation of Envisat and CryoSat-2 SIT with respect to the reference observations provides consistent results:

1. The SIT bias for both platforms is negative, indicating thinner sea ice in the CDR compared to the validation data. The bias of Envisat (-0.62 m) is larger than the bias of CryoSat-2 (-0.11 m).
2. Overall Envisat uncertainty (RMSE) is higher (0.72 m) than CryoSat-2 (0.58 m).
3. RMSE values derived from airborne data are larger than RMSE values derived from ULS data. A potential explanation is a better representativeness of the ULS data (RMSE of 0.55 m for Envisat and 0.23 m for CryoSat-2). Airborne data coverage is non-uniform for all grid cells and typically only covers 1 day of the monthly periods. Uncertainties derived from airborne EM data therefore potentially inflated by uncertainty of the validation data.

It must be noted that this thickness evaluation is very regionalised and in the case of the AEM data limited to the spring months of March and April. Different results are likely to be obtained in other regions if validation data would be available.

1.2.2 Sea Ice Thickness Precision

Another metric can be used to verify the internal consistency of the SIT retrieval on daily scales: Along-track averages of SIT information within 25 km of cross-over ground points from the same satellite on a calendar day, indicate the precision of one orbit segment in the size of a Level-3 grid cell [D1].

Table 10: Thickness Differences for daily crossovers of Envisat (2002-2012) and CryoSat-2 (2010-2020).

Platform	Crossovers (number)	Mean difference (m)	Mean absolute difference (m)
Envisat	80747	-0.002	0.36
CryoSat-2	175661	-0.003	0.33

The results of the internal cross-over analysis are presented in Table 10 with mean thickness difference and mean absolute difference as the main metric for estimating SIT precision at a scale of 25 km. The precision of both Envisat and CryoSat-2 show only a minimal difference of 3 cm in total.
But while the statistics are based on a robust number of crossovers, the mean absolute SIT difference is impacted by the orbit configuration, which controls the geographic location of daily crossovers and thus sea ice conditions. The mean absolute difference is smaller in regions with thinner sea ice, and Envisat crossovers are generally located at lower latitudes with thinner ice than most CryoSat-2 crossovers that are located at high latitudes in the central Arctic. A fairer comparison would likely result in a larger precision difference, nevertheless the precision of Envisat is a considerable improvement with respect to version 2.0 of the SIT CDR.

1.2.3 Time Series Stability

The stability requirement for CDRs is essential when the observations are based on different satellite missions with developing/improving sensor specifications. This is the case for the change from pulse-limited radar altimeter onboard Envisat to the synthetic aperture radar of CryoSat-2 with improved spatial resolution. An additional factor for product stability is temporal changes in the fidelity of auxiliary parameters.

1.2.3.1 Intermission Bias

The introduction of the synthetic aperture radar altimeter SIRAL of the CryoSat mission poses a significant change in sensor characteristics for the SIT CDR period. The main impacts are:

1. Significantly reduced sensor footprint,
2. Different sensitivity of waveforms to surface roughness.

As a result, different algorithms are required for surface type classification and ranging. These algorithms need to compensate for preferential sampling of high backscatter targets, e.g., thin ice or leads, to achieve stability between the two radar altimeter generations. Otherwise, significant inconsistencies can be observed (Schwegmann et al., 2016).

The thickness bias however is not uniform across months (Table 11) or thickness categories, with the general tendency of Envisat thick ice being biased low and thin ice being biased high with respect to CryoSat-2. Similar results are obtained when validating Envisat- and CryoSat-2-derived thickness with independent reference data (Section 1.2.1).

Table 11: CryoSat-2 – Envisat basin scale SIT bias for different reference periods.

Reference period	CryoSat-2 – Envisat thickness bias
October (2011)	0.03 m
November (2010, 2011)	-0.03 m
December (2010, 2011)	-0.03 m
January (2011, 2012)	-0.02 m
February (2011, 2012)	-0.06 m
March (2011, 2012)	-0.05 m
April (2011)	-0.08 m
All Months	-0.03 m

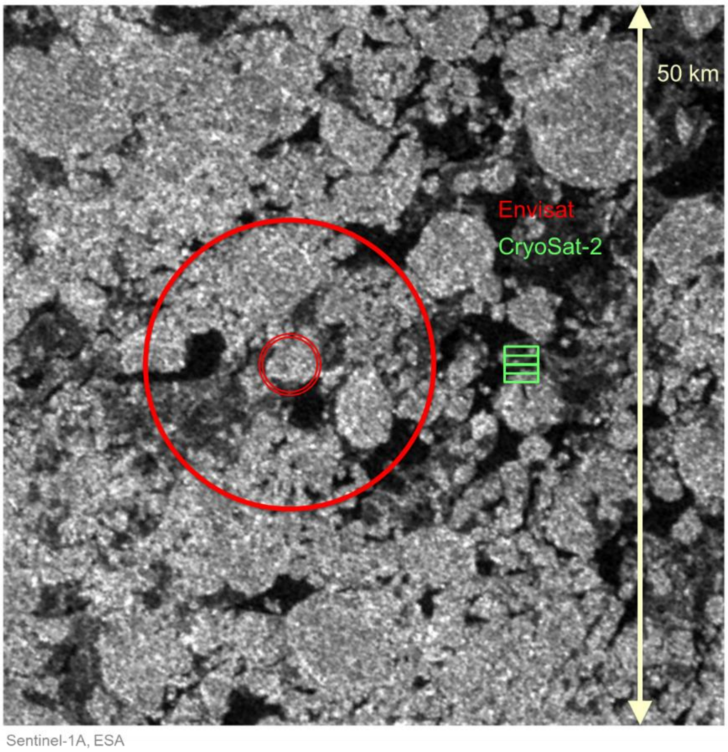

Figure 5: Sensor footprint characteristics for Envisat (specular backscatter targets: outer circle, diffuse backscatter targets: inner circle) and CryoSat-2 (1 rectangle).

The comparison to the reference data indicates an additional limitation for the data record stability for the Envisat period. A linear trend fitted to the mean monthly difference between the satellite and reference data indicated a trend of approximately 5 cm per year. It is evident that early Envisat SIT data is too thin with respect to reference data, especially pre-2008. This issue is independent of the Envisat/CryoSat-2 intermission biases and its sources are currently under investigation.

In any case, SIT trends computed from the CDR/ICDR are highly likely to be biased low compared to the real trends. This holds at least in the Beaufort Sea where the longest record of reference data exists.

1.2.3.2 Snow Depth Climatology

The snow climatology (see section 1.1.3.3) does not contain any trends or interannual variability in its static monthly snow depth fields. The ice type dependent snow depth modification does cause a change of mean snow depth in the SIT retrieval algorithm that is linearly dependent on the fraction of first-year ice area. However, its relation to true Arctic snow depth trends and variability is still poorly understood.

It has been shown by Mallett et al. 2021 that using dynamic snow load increases the trends, and variability, of sea ice thickness climate data records in the marginal seas.

1.3 Data usage information

1.3.1 Product Specification

Data from the Level-3 SIT CDR/ICDR are available in netCDF-4 format following the Climate & Forecast (CF) conventions version 1.7 and Attribute Convention for Data Discovery version 1.3.

A graphical overview of the main variables and corresponding flags is given in Figure 6.

The filename of each monthly netCDF file indicates the type of CDR and data period:

ice_thickness_nh_ease2-250_<cdr|icdr>-v3p0_<yyyy><mm>.nc

The main metadata of the Level-3 file is stored in the global attributes (Table 12) of the product:

Table 12: Global attributes of each monthly Level-3 sea ice thickness product.

<table>
<tr><th>Attribute</th><th>Value</th></tr>
<tr><td>title</td><td>Sea ice thickness</td></tr>
<tr><td>institution</td><td>Alfred-Wegener-Institut Helmholtz Zentrum für Polar und Meeresforschung</td></tr>
<tr><td>source</td><td>Altimetry: Cryosat-2, Snow depth: Monthly climatology based on regional merging of Warren Climatology with 50% reduction for first-year sea ice in the central Arctic and AMSR-2 based snow depth from IUP Bremen in remaining ice-covered regions, Mean Sea Surface: DTU21 global mean sea surface, Sea ice Concentration: C3S Sea Ice Concentration CDR v3p0, Sea ice type: C3S Sea Ice Type CDR v3p0"</td></tr>
<tr><td>platform</td><td><Envisat|CryoSat-2></td></tr>
<tr><td>sensor</td><td><RA-2|SIRAL></td></tr>
<tr><td>history</td><td>yyyymmddThhmissZ (created)</td></tr>
<tr><td>references</td><td>Product User Guide and Specification (PUGS): SIT Version 3, Algorithm Theoretical Baseline Document (ATBD): SIT Version 3</td></tr>
<tr><td>tracking_id</td><td>Unique identifier string (e.g. f25214d1-d727-44d9-b50f-32ed24c0f4b0)</td></tr>
<tr><td>Conventions</td><td>CF-1.7 ACDD-1.3</td></tr>
<tr><td>product_version</td><td>3p0</td></tr>
<tr><td>processing_level</td><td>Level-3 Collated (l3c)</td></tr>
<tr><td>summary</td><td>Monthly gridded Northern Hemisphere SIT Climate Data Record (CDR) from Envisat and CryoSat-2 satellite radar altimetry for the period October 2002 - April 2020</td></tr>
<tr><td>keywords</td><td>GCMDSK:Earth Science > Cryosphere > Sea Ice > Ice Depth/Thickness, GCMDSK:Earth Science > Oceans > Sea Ice > Ice Depth/Thickness, GCMDSK:Earth Science > Climate Indicators > Cryospheric Indicators > Ice Depth/Thickness, GCMDLOC:Geographic Region > Northern Hemisphere, GCMDLOC:Vertical Location > Sea Surface, GCMDPROV:Consortia/Institutions > AWI > Alfred Wegener Institute for Polar and Marine Research</td></tr>
</table>

Table 12 (continued): Global attributes of each monthly Level-3 sea ice thickness product.

Attribute	Value
keywords_vocabulary	GCMDSK:GCMD Science Keywords:https://gcmd.earthdata.nasa.gov/kms/concepts/concept_scheme/sciencekeywords, GCMDLOC:GCMD Locations:https://gcmd.earthdata.nasa.gov/kms/concepts/concept_scheme/locations, GCMDPROV:GCMD Providers:https://gcmd.earthdata.nasa.gov/kms/concepts/concept_scheme/providers
id	c3s-sit-<cdr|icdr>-v3p0-l3c-<envisat|cryosat2>-nh25kmEASE2-yyyymm
naming_authority	de.awi
keywords_vocabulary	GCMD Science Keywords
doi	
cdm_data_type	grid
comment	Northern hemisphere SIT coverage is limited to the winter month between October and April due to negative effect of surface melt on the retrieval of freeboard. Please consult the Product User Guide and Specifications (PUGS) for more information.
date_created	yyyymmddThhmissZ
creator_name	Alfred-Wegener-Institut Helmholtz Zentrum für Polar und Meeresforschung
creator_type	institution
creator_url	http://www.awi.de
creator_email	stefan.hendricks@awi.de
project	Copernicus Climate Change Services (C3S)
contributor_name	Stefan Hendricks, Robert Ricker, Stephan Paul, Eero Rinne, Heidi Sallila
contributor_role	PrincipalInvestigator, Author, Author, Author, Author
publisher_name	Copernicus Climate Data Store
publisher_url	https://climate.copernicus.eu/climate-data-store
publisher_email	copernicus-support@ecmwf.int
geospatial_lat_min	16.6239
geospatial_lat_max	90.0
geospatial_lon_min	-180.0
geospatial_lon_max	180.0
geospatial_vertical_min	0.0

Table 12 (continued): Global attributes of each monthly Level-3 sea ice thickness product.

Attribute	Value
geospatial_vertical_max	0.0
spatial_resolution	25.0 km grid spacing
geospatial_bounds_crs	EPSG:6931
time_coverage_start	"2015-03-01T00:00:00"
time_coverage_end	"2015-03-31T23:59:59.999999"
time_coverage_duration	P1M
time_coverage_resolution	P1M
standard_name_vocabulary	CF Standard Name Table (v36, 21 September 2016)
license	C3S Copernicus License (see https://cds-dev.copernicus-climate.eu/api/v2/terms/static/20180314_Copernicus_License_V1.1.pdf)

Each file contains several variables that contain the main geophysical parameter and its uncertainty (sea_ice_thickness; uncertainty) as well as data flags and variables describing the reference time, period, and the geographical location of each grid cell (Table 13).

Table 13: Variables contained in each monthly Level-3 SIT product dataset.

Name	Type	Dimension	Description
quality_flag	Byte	time, yc, xc	Retrieval quality flag (see below)
sea_ice_thickness	float	time, yc, xc	Main geophysical parameter
status_flag	byte	time, yc, xc	Retrieval status flag (see below)
uncertainty	float	time, yc, xc	Uncertainty of geophysical parameter
time_bnds	double	time, 2	Time range of period
Lambert_Azimuthal_Grid	byte	None	Grid definition
lat	double	yc, xc	Latitude coordinate
lon	double	yc, xc	Latitude coordinate
time	double	time	Reference time
xc	double	xc	x coordinate of projection
yc	double	Yc	y coordinate of projection

1.3.1.1 Flags

Each file contains two types of status flags for the SIT retrieval. The regular status flag (variable: status_flag) indicates the general result of the retrieval process, and can take the following values for each grid cell (bit value: meaning):

0: Nominal retrieval

1: No data

2: Open ocean

3: Satellite pole hole

4: Land, lake, or land ice

5: Retrieval failed

The additional quality indicator flag is only available for grid cells with successful retrieval (status_flag = 0). It adds an additional expert guess of retrieval outcome in three categories (bit value: meaning):

0: Nominal quality

1: Intermediate quality

2: Low quality

3: No data

The computation of the quality flag is based on a set of rules and grid cell statistics, shown in Table 14.

Table 14: Criterias for Level-3 quality assessment categories.

Quality Assessment	Criterion
Low	Less than 10 Level-2 thickness data points per grid cell
Low	Negative thickness fraction > 40%
Low	Median of marginal ice zone filter flag value is 2
Intermediate	CryoSat-2 in SIN mode (CryoSat-2 specific)
Intermediate	Area lead fraction (the maximum lead fraction in grid cells with 75 km search radius) < 10%
Intermediate	Less than 50 Level-2 thickness data points per grid cell
Intermediate	Negative thickness fraction between 20% - 40%
Intermediate	Median of marginal ice zone filter flag value is 1
Nominal	None of the above

1.3.1.2 Projection and Grid Specification

The projection is defined as the Equal-Area Scalable Earth Grid version 2 (EASE2-Grid) (Brodzik et al., 2012) for the northern hemisphere with a resolution of 25km.

Table 15: Key properties of the EASE2-Grid projection used for Level-3 northern hemisphere sea ice products.

Property	**Value**
false_easting	0.0
false_northing	0.0
grid_mapping_name	lambert_azimuthal_equal_area
inverse_flattening	298.257223563
latitude_of_projection_origin	90.0
longitude_of_projection_origin	0.0
proj4_string	+proj=laea +lon_0=0 +datum=WGS84 +ellps=WGS84 +lat_0=90.0
semi_major_axis	6378137.0

Table 16: Grid extent and spacing for Level-3 northern hemisphere sea ice products.

Property	**Value**
Grid Dimension	(432, 432)
Grid Spacing (km)	25.0
Grid Notation	Center Coordinates
Grid x extent in projection coordinates (km)	(-5387.5, 5387.5)
Grid y extent in projection coordinates (km)	(-5387.5, 5387.5)

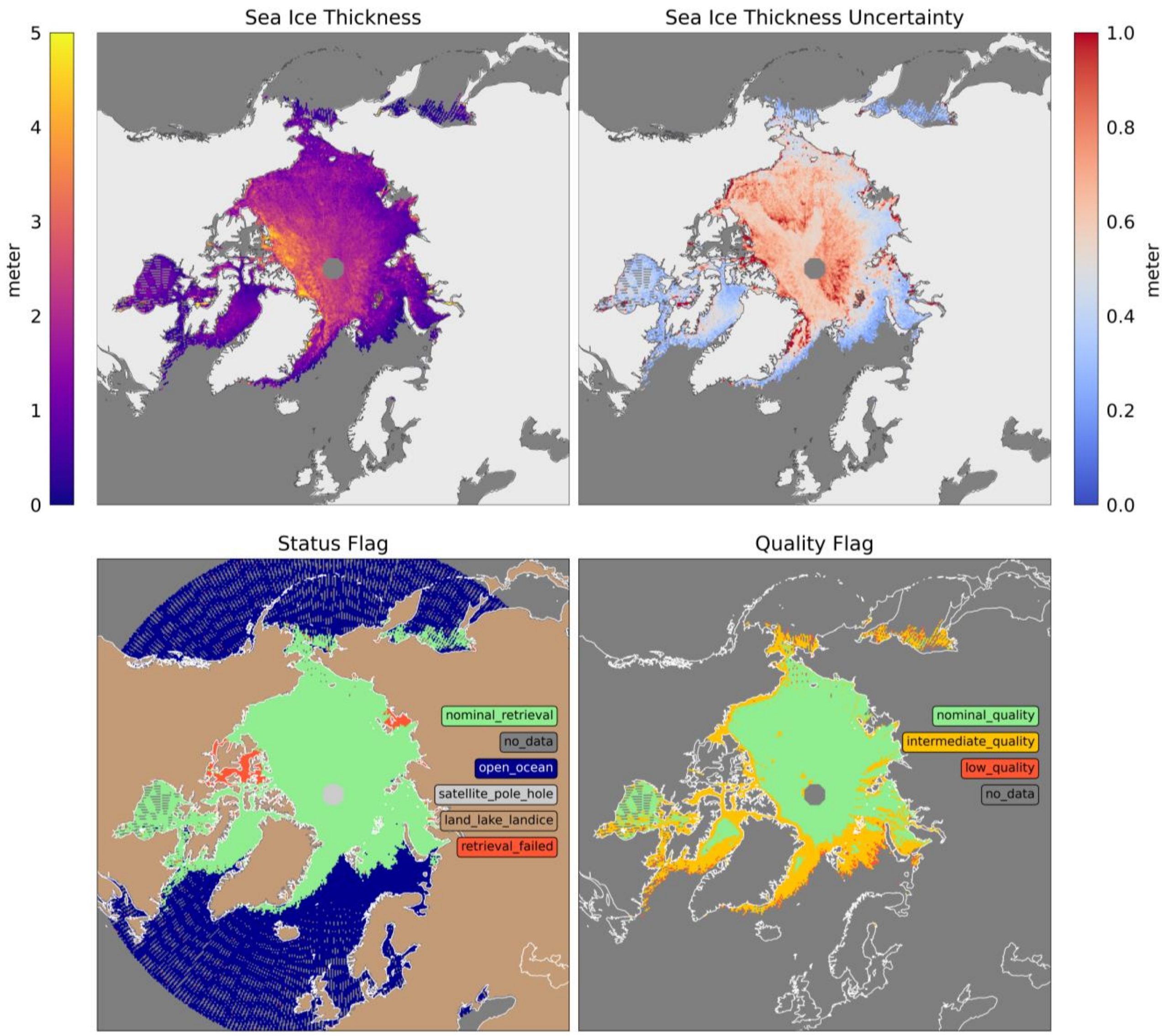

Figure 6: Content the C3S SIT CDR/ICDR files. Four different data layers in sample dataset (ice_thickness_nh_ease2-250_cdr-v3p0_202004.nc) are shown. Top row: gridded sea ice thickness (left) and its uncertainty (right). Bottom row: Status flag (left) and quality flag (right) of the retrieval.

1.3.2 Known Issues

Various components of the SIT retrieval algorithm are an active field of research with expected improvements in upcoming product versions. Without claim of completeness, these fields of research include:

1. Ranging over sea ice surfaces with varying snow depth, stratigraphy, and surface roughness.
2. Estimation of instantaneous sea surface height in the marginal ice zone, with low wave heights and continuity to open ocean sea surface height observations
3. Estimation of snow depth and density from re-analysis with realistic interannual and decadal variability.

These topics touch on various aspects of the SIT retrieval and will be included in future product developments. This section therefore provides an overview of the known issues and limitations of the current algorithm and auxiliary data sets.

1.3.2.1 Snow Backscatter

A key assumption in the ranging algorithm over snow covered sea ice is that the main scattering horizon is the ice/snow interface for sea ice conditions between October and April in the northern hemisphere. There is however ample evidence in the scientific literature that backscatter from the snow layer can influence radar ranging with Ku-Band frequencies (e.g., Kurtz et al., 2014; Kwok R., 2014; Ricker et al., 2015; Nandan et al., 2017).

Snow backscatter causes the freeboard to be biased high and thus leads to an overestimation of SIT. The ranging algorithm used for the C3S SIT CDR/ICDR is empirical, without snow depth as an input parameter. However, the geometric correction used for converting the radar-derived freeboard into sea ice freeboard depends on snow depth and is an obvious candidate for including snow backscatter related range biases. Currently, little is known about the temporal and spatial variability of this effect and a basin scale parametrization requires an extensive and dedicated observational program.

The bias of CryoSat-2 results with respect to validation data is well within the uncertainties of the auxiliary parameters, and Envisat is biased low. Thus, we do not expect a significant and widespread snow backscatter bias to be present, however regional thicknesses might be biased high.

1.3.2.2 Sea Ice Thickness Trends

The observed intermission bias, the generally lower performance of the Envisat SIT data, and the unvarying snow load need to be considered when computing trends of sea ice thickness from the entire C3S CDR. It is highly likely that any trends computed from the C3S CDR are biased low.

2. Data access information

2.1 Product Download

The data products are available and can be downloaded through the C3S Climate Data Store (CDS) under the dataset entitled "*Sea ice thickness monthly gridded data for the Arctic from 2002 to present derived from satellite observations*":

https://cds.climate.copernicus.eu/cdsapp#!/dataset/satellite-sea-ice-thickness

2.2 Visualization Tools

2.2.1 CDS Toolbox

The CDS toolbox (https://cds.climate.copernicus.eu/toolbox-editor) enables users to create custom applications based on CDS data in a web browser. The toolbox utilizes the python-based module cdstoolbox, which can be used to extract and analyze data as well as create interactive maps.

The CDS toolbox also enables users to visualize sea ice thickness data, as illustrated in the example below (Figure 7).

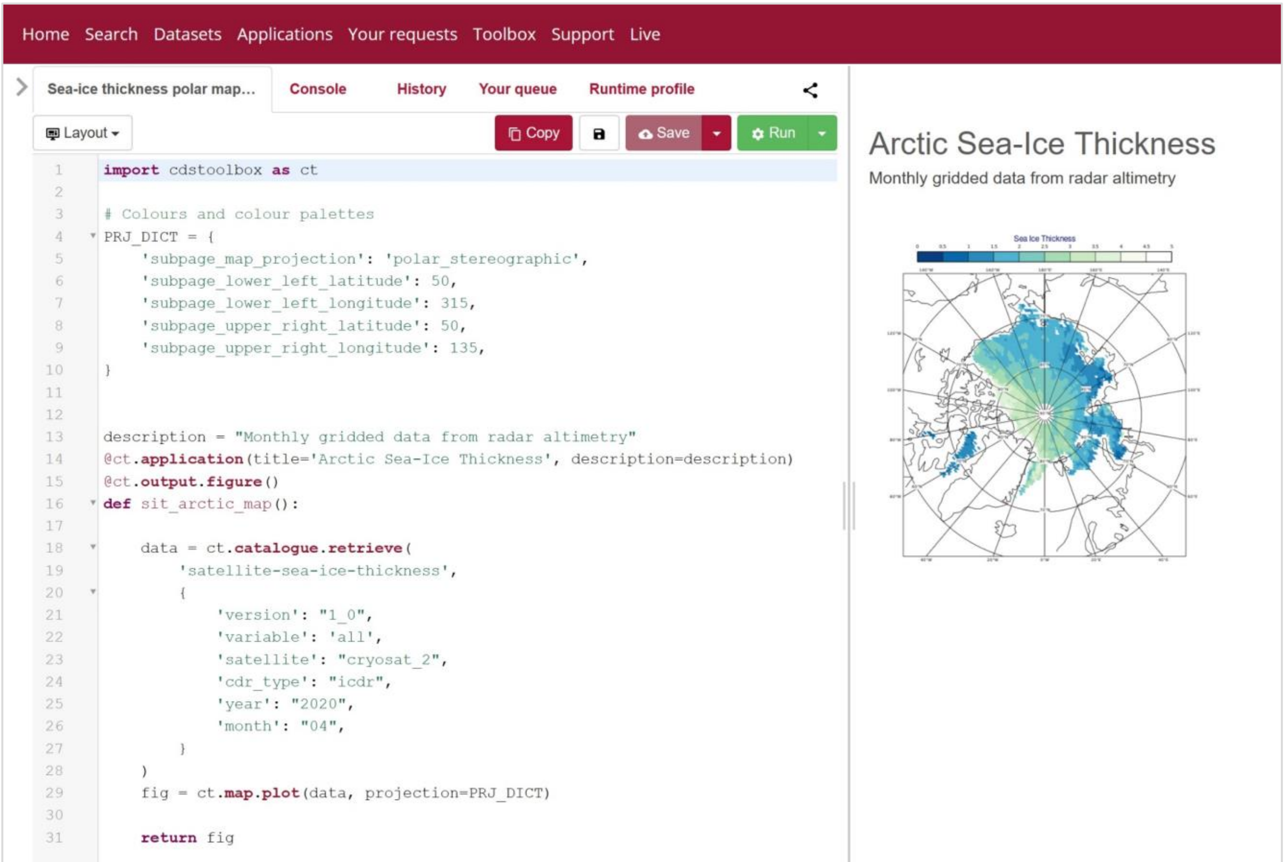

Figure 7: Example visualization of the monthly gridded sea ice thickness field for April 2020, using the CDS toolbox.

2.2.2 Panoply

The NASA Panoply netCDF, HDF and GRIB data viewer (https://www.giss.nasa.gov/tools/panoply/) can be used as an offline viewer and is available for multiple platforms. See Figure 8 for an example.

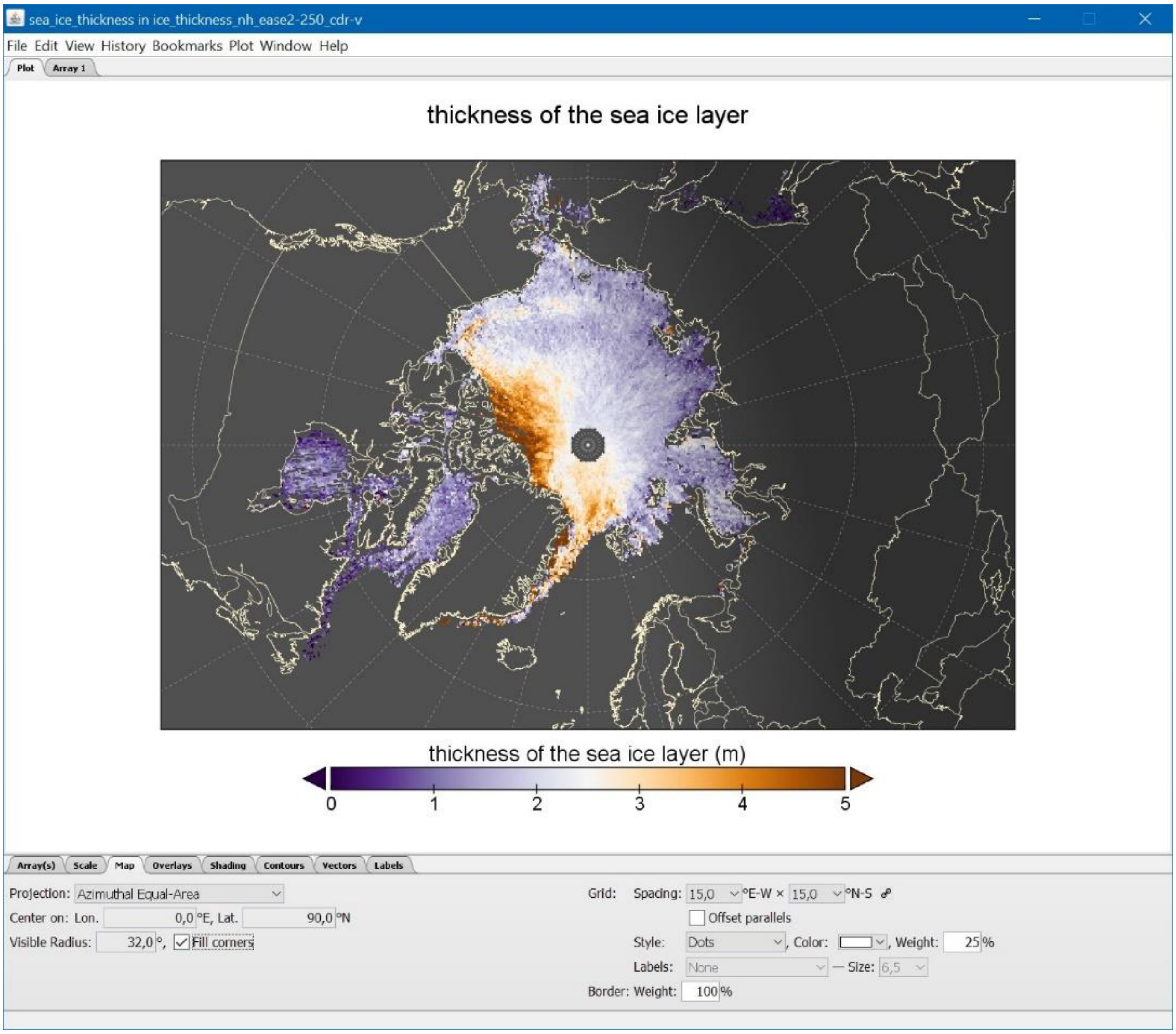

Figure 8: Data visualization example with panoply data viewer from NASA.

2.3 Point of Contact

Please contact the Copernicus User Service Desk

Table 17: Points of contact for product and data access related issues.

Contact	ECMWF Support Portal (https://confluence.ecmwf.int/site/support)

3. Appendix A - Specifications for Sea Ice Thickness

Property	Value
Algorithm	C3S v3.0 (derived from CCI v3.0)
Platforms	Envisat; CryoSat-2
Period	October 2002 – April 2020 CDR (v3.0) Envisat: October 2002 – October 2010 CryoSat-2: November 2010 – April 2020 (CDR) October 2020 and ongoing (ICDR)
Coverage	Northern Hemisphere Envisat: Latitude > 81.45N CryoSat-2: Latitude > 88.0N
Temporal Resolution	Monthly
Timeliness (ICDR)	1 Month
Spatial Resolution	25 km
Grid Projection	EASE2 Northern Hemisphere (Lambert Azimuthal Equal Area) (+proj=laea +lon_0=0 +datum=WGS84 +ellps=WGS84 +lat_0=90.0)
Data Gaps	May – September (melting season)
Product File Format	netCDF-v4 Climate & Forecast conventions
Product Variables	sea ice thickness sea ice thickness algorithm uncertainty status flag quality flag

4. References

Alexandrov, V., Sandven, S., Wahlin, J., and Johannessen, O. M.: The relation between sea ice thickness and freeboard in the Arctic, The Cryosphere, 4, 373-380, https://doi.org/10.5194/tc-4-373-2010, 2010.

Brodzik, M. J., Billingsley, B., Haran, T., Raup, B., and Savoie, M. H.: EASE-Grid 2.0: Incremental but Significant Improvements for Earth-Gridded Data Sets, ISPRS International Journal of Geo-Information, 1, 32–45, doi:10.3390/ijgi1010032, URL http://www.mdpi.com/2220-9964/1/1/32, 2012.

Guerreiro, K., Fleury, S., Zakharova, E., Kouraev, A., Rémy, F., and Maisongrande, P.: Comparison of CryoSat-2 and ENVISAT radar freeboard over Arctic sea ice: toward an improved Envisat freeboard retrieval, The Cryosphere, 11, 2059-2073, https://doi.org/10.5194/tc-11-2059-2017, 2017.

Jutila, A., King, J., Paden, J., Ricker, R., Hendricks, S., Polashenski, C., Helm, V., Binder, T. and Haas, C. (2021a): High-Resolution Snow Depth on Arctic Sea Ice From Low-Altitude Airborne Microwave Radar Data, IEEE TGRS, pp. 1-16. doi: 10.1109/TGRS.2021.3063756

Jutila, A., Hendricks, S., Ricker, R., von Albedyll, L., Krumpen, T., and Haas, C.: Retrieval and parametrisation of sea-ice bulk density from airborne multi-sensor measurements, The Cryosphere Discuss. [preprint], https://doi.org/10.5194/tc-2021-149, in review, 2021b.

Kurtz, N. T., and S. L. Farrell (2011), Large-scale surveys of snow depth on Arctic sea ice from Operation IceBridge, Geophys. Res. Lett., 38, L20505, doi:10.1029/2011GL049216.

Kurtz, N. T., Galin, N., and Studinger, M.: An improved CryoSat-2 sea ice freeboard retrieval algorithm through the use of waveform fitting, The Cryosphere, 8, 1217-1237, https://doi.org/10.5194/tc-8-1217-2014, 2014.

Kwok, R. (2014), Simulated effects of a snow layer on retrieval of CryoSat‐2 sea ice freeboard, Geophys. Res. Lett., 41, 5014–5020, doi: 10.1002/2014GL060993.

Lavergne, T., Kern, S., Aaboe, S., Derby, L., Dybkjaer, G., Garric, G., Heil, P., Hendricks, S., Holfort, J., Howell, S., Key, J., Lieser, J. L., Maksym, T., Maslowski, W., Meier, W., Muñoz-Sabater, J., Nicolas, J., Özsoy, B., Rabe, B., Rack, W., Raphael, M., de Rosnay, P., Smolyanitsky, V., Tietsche, S., Ukita, J., Vichi, M., Wagner, P., Willmes, S., & Zhao, X. (2022). A New Structure for the Sea Ice Essential Climate Variables of the Global Climate Observing System, Bulletin of the American Meteorological Society, 103(6), E1502-E1521. Retrieved Feb 21, 2023, from https://journals.ametsoc.org/view/journals/bams/103/6/BAMS-D-21-0227.1.xml

Laxon, S., Peacock, N., and Smith, D.: High interannual variability of sea ice thickness in the Arctic region, Nature, 425, 947–950, 2003.

Mallett, R. D. C., Lawrence, I. R., Stroeve, J. C., Landy, J. C., and Tsamados, M.: Brief communication: Conventional assumptions involving the speed of radar waves in snow introduce systematic underestimates to sea ice thickness and seasonal growth rate estimates, The Cryosphere, 14, 251–260, https://doi.org/10.5194/tc-14-251-2020, 2020.

Mallett, R. D. C., Stroeve, J. C., Tsamados, M., Landy, J. C., Willatt, R., Nandan, V., and Liston, G. E.: Faster decline and higher variability in the sea ice thickness of the marginal Arctic seas when accounting for dynamic snow cover, The Cryosphere, 15, 2429–2450, https://doi.org/10.5194/tc-15-2429-2021, 2021.

Nandan, V., Geldsetzer, T., Yackel, J., Mahmud, M., Scharien, R., Howell, S., … Else, B. (2017). Effect of snow salinity on CryoSat‐2 Arctic first‐year sea ice freeboard measurements. Geophysical Research Letters, 44, 10,419–10,426.

Paul, S., Hendricks, S., Ricker, R., Kern, S., and Rinne, E.: Empirical parametrization of Envisat freeboard retrieval of Arctic and Antarctic sea ice based on CryoSat-2: progress in the ESA Climate Change Initiative, The Cryosphere, 12, 2437–2460, https://doi.org/10.5194/tc-12-2437-2018, 2018.

Stephan Paul, & Stefan Hendricks. (2022). Feed-Forward Neural Network for ENVISAT Retracker Threshold Computation (v1.0). Zenodo. https://doi.org/10.5281/zenodo.7436473

Ricker, R., S. Hendricks, D. K. Perovich, V. Helm, and R. Gerdes (2015), Impact of snow accumulation on CryoSat-2 range retrievals over Arctic sea ice: An observational approach with buoy data. Geophys. Res. Lett., 42, 4447–4455. doi: 10.1002/2015GL064081.

Schwegmann, S., Rinne, E., Ricker, R., Hendricks, S., and Helm, V.: About the consistency between Envisat and CryoSat-2 radar freeboard retrieval over Antarctic sea ice, The Cryosphere, 10, 1415-1425, https://doi.org/10.5194/tc-10-1415-2016, 2016.

*Warren, S.G., I.G. Rigor, N. Untersteiner, V.F. Radionov, N.N. Bryazgin, Y.I. Aleksandrov, and R. Colony, 1999: Snow Depth on Arctic Sea Ice. J. Climate, **12**, 1814–1829*

WMO (World Meteorological Organization, The 2022 GCOS ECVs Requirements (GCOS 245), 2022, https://library.wmo.int/doc_num.php?explnum_id=11318